

Stable Blue Thermally Activated Delayed Fluorescent Organic Light-Emitting Diodes with Three Times Longer Lifetime than Phosphorescent Organic Light-Emitting Diodes

Mounggon Kim, Sang Kyu Jeon, Seok-Ho Hwang, and Jun Yeob Lee*

Thermally activated delayed fluorescent (TADF) devices are attractive as next-generation high efficiency organic light-emitting diodes (OLEDs) because of potential internal quantum efficiency of 100% by utilizing both singlet and triplet excitons for singlet emission. In reality, high internal quantum efficiency close to 100% has already been released in green TADF devices by doping (4s,6s)-2,4,5,6-tetra(9H-carbazol-9-yl) (4CzIPN) in a mixed host-emitting layer structure.^[1] Currently, the best maximum quantum efficiency of green TADF devices is 29.6% and that of blue TADF devices is 19.5%.^[2,3] Therefore, the TADF devices are gathering more attention as high efficiency OLEDs.

Although a significant progress of the quantum efficiency of the green and blue TADF OLEDs has been made for the last couple of years through the development of host and dopant materials for TADF devices,^[4–14] there have been only a few papers about the stability of the TADF devices and all of them investigated the lifetime of the 4CzIPN-doped TADF OLEDs. Adachi and co-workers^[15] performed comprehensive study about the stability of the green TADF OLEDs and concluded that the lifetime of the green TADF OLEDs is similar to that of green phosphorescent OLEDs. Our group also compared the lifetime of the green TADF OLEDs with that of green phosphorescent OLEDs and reported analogous lifetime in the two devices.^[16] However, there has been no work reporting the lifetime of the blue TADF OLEDs possibly due to poor stability of the blue TADF emitters developed so far. 10,10'-(Sulfonylbis(4,1-phenylene))bis(9,9-dimethyl-9,10-dihydroacridine) (DMAC-DPS) was a highly efficient blue TADF emitter, but it was not stable at all by a highly polar diphenylsulfone moiety in the backbone structure. Other than DMAC-DPS, several blue TADF materials such as 2-biphenyl-4,6-bis(12-phenylindolo[2,3-a]carbazole-11-yl)-1,3,5-triazine^[4] and bis[4-(3,6-di-tert-butylcarbazole)phenyl]sulfone^[9] were prepared, but stability of the blue

TADF OLEDs was not mentioned. Therefore, there is a strong demand for the development of high efficiency and stable blue TADF OLEDs via stable TADF emitter design.

Here, design, synthesis, comprehensive material characterization, and device characterization of blue TADF emitters derived from a dicarbazolylbenzene donor and a triazine acceptor are described. Two deep blue TADF emitters, 9,9'-(5-(4,6-diphenyl-1,3,5-triazin-2-yl)-1,3-phenylene)bis(9H-carbazole) (DCzTrz) and 9,9',9'',9'''-((6-phenyl-1,3,5-triazine-2,4-diyl)bis(benzene-5,3,1-triyl))tetrakis(9H-carbazole) (DDCzTrz), accomplished a high quantum efficiency of 18.9% and lifetime up to 80% of initial luminance of 52 h at an initial luminance of 500 cd m⁻² as blue TADF emitters. The lifetime of the blue TADF OLEDs with the DDCzTrz was almost tripled compared to that of blue phosphorescent OLEDs with an Ir-based triplet emitter derived from a stable phenylimidazole ligand, which suggests that the molecular structure based on triazine and dicarbazolylbenzene has a potential as a backbone structure for the development of stable blue TADF OLEDs. This work is a first demonstration of the blue TADF devices with a better lifetime than blue triplet devices.

In order to develop stable blue TADF emitters, they should be designed to contain only stable donor and acceptor moieties in the molecular structure. In the case of the donor moieties, carbazole was chosen because it is potentially better than other moieties such as acridine and phenoxazine in terms of stability. Carbazole is made up of only aromatic moieties with high bond dissociation energy, while other moieties have less stable sp³ bond with low dissociation energy. Carbazole was also proven to be stable as a moiety of host materials such as 3,3-di(9H-carbazol-9-yl)biphenyl (mCBP). In the case of the acceptor moieties, diphenylsulfone, phthalonitrile, and triazine have been reported and triazine was selected as the stable acceptor moiety because of aromatic character of the triazine moiety. Therefore, two TADF emitters were constructed to have the triazine and carbazole units. The carbazole units were introduced as a dicarbazolylphenyl form to weaken the donor strength of the carbazole units because the emission color can be controlled by the donor and acceptor strength of the molecule. For deep blue emission, weak donors are preferable because the singlet energy stabilization effect is less significant by weak charge transfer (CT) character. One or two dicarbazolylphenyl units were attached to the triazine core to control the emission color.

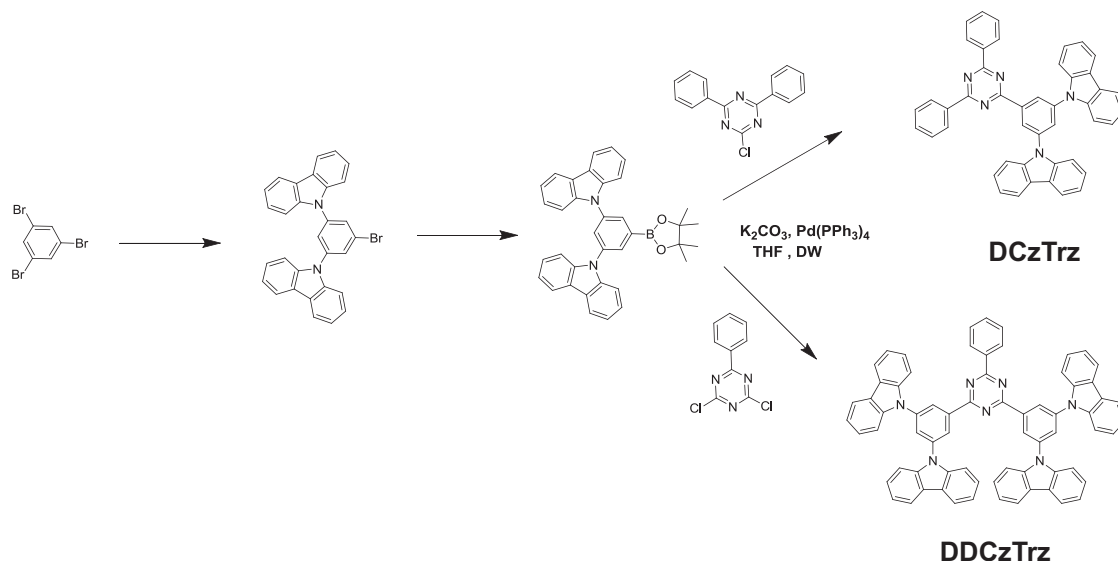
Synthetic scheme of DCzTrz and DDCzTrz is shown in Scheme 1. Suzuki-coupling reaction of boronic ester of

M. Kim, Prof. S.-H. Hwang
Department of Polymer Science and Engineering
Dankook University
126, Jukjeon-dong, Suji-gu, Yongin,
Gyeonggi 448–701, Korea

S. K. Jeon, Prof. J. Y. Lee
School of Chemical Engineering
Sungkyunkwan University
2066, Seobu-ro, Jangan-gu, Suwon, Gyeonggi 440–746, Korea
E-mail: lee17@skku.edu



DOI: 10.1002/adma.201500267



Scheme 1. Synthetic scheme of DCzTrz and DDCzTrz.

dicarbazolylbenzene with 2-chloro-4,6-diphenyl-1,3,5-triazine and 2,4-dichloro-6-phenyl-1,3,5-triazine produced DCzTrz and DDCzTrz, respectively. Synthesis yields of DCzTrz and DDCzTrz were 91% and 85%, respectively.

Molecular orbital calculation of DCzTrz and DDCzTrz was performed to simulate the highest occupied molecular orbital (HOMO) and the lowest unoccupied molecular orbital (LUMO)

because the molecular orbital can be correlated with the photophysical properties of the compounds. **Figure 1a** represents the HOMO and LUMO distribution of DCzTrz and DDCzTrz. There was little discrepancy of the HOMO and LUMO distribution between DCzTrz and DDCzTrz, and the HOMO dispersion on the dicarbazolylphenyl moiety and the LUMO spreading on the triazine moiety were apparent by the donor–acceptor

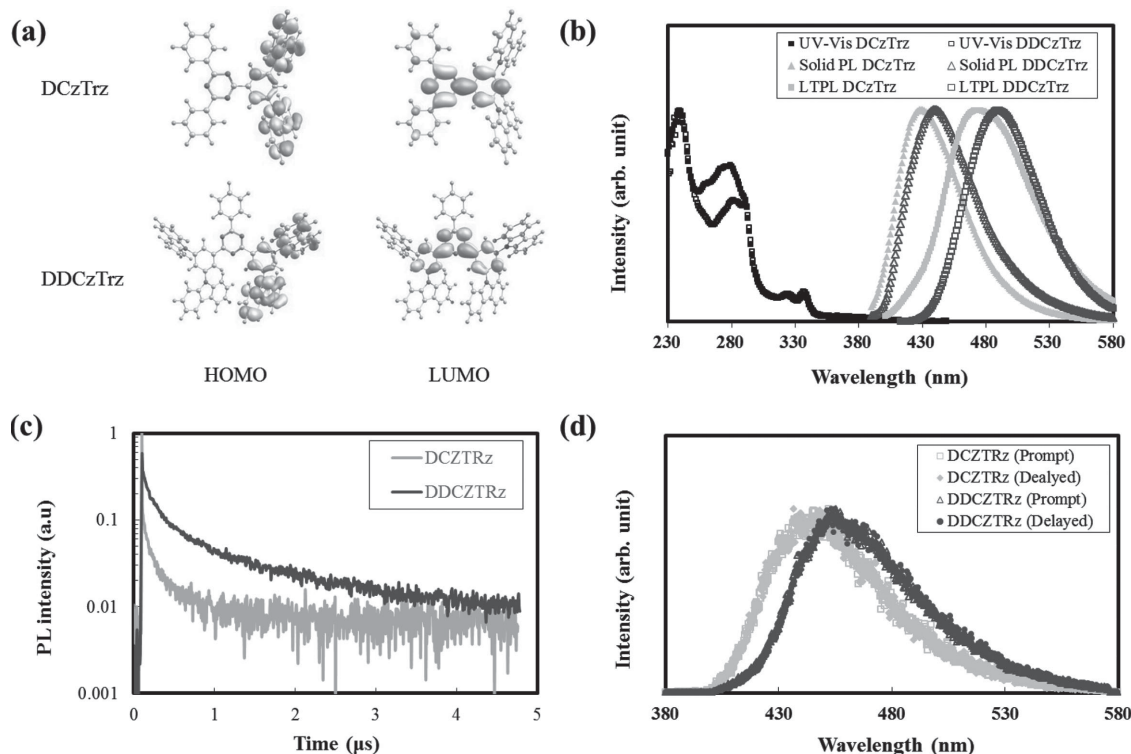


Figure 1. HOMO and LUMO distribution of DCzTrz and DDCzTrz calculated using B3LYP/6–31G* basis set of Gaussian 09 program (a). Solution UV–vis, solution PL, and low-temperature PL spectra in tetrahydrofuran of DCzTrz and DDCzTrz (b). Transient PL decay curves (c) and time-resolved PL spectra of DCzTrz and DDCzTrz (d).

character of the TADF emitters. The overlap of the HOMO and LUMO was also found in the phenyl unit of dicarbazolylphenyl moiety. Therefore, the DCzTrz and DDCzTrz emitters possessed an appropriate molecular orbital distribution of the TADF emitters with extensively isolated HOMO/LUMO for small singlet–triplet energy gap and weakly overlapped HOMO/LUMO for efficient light emission.

The HOMO and LUMO distribution is reflected in the photophysical properties of the TADF emitters and the ultraviolet-visible (UV–vis) and photoluminescence (PL) analysis results are presented in Figure 1b. UV–vis absorption spectra of DCzTrz and DDCzTrz were similar each other except for the slight red shift of the absorption peak. Absorption edge of DCzTrz and DDCzTrz could reach 411 and 412 nm, respectively. In contrast to the similar UV–vis absorption spectra, large shift of PL emission spectra in solid polystyrene to long wavelength was detected in DDCzTrz. Singlet emission energy of DDCzTrz was 2.80 eV, which was lower than that of DCzTrz (2.89 eV) by 0.09 eV due to strengthened donor character by two dicarbazolylphenyl moieties. Triplet energy of DDCzTrz (2.53 eV) was also lowered by 0.11 eV compared to that of DCzTrz (2.64 eV) due to extended conjugation by the additional dicarbazolylphenyl moiety. Singlet–triplet energy gaps of DCzTrz and DDCzTrz were 0.25 and 0.27 eV, respectively. In the PL measurement, strong solvatochromic effect was observed by CT character of excited state caused by donor–acceptor structure of DCzTrz and DDCzTrz. Solvent-dependent PL spectra of DCzTrz and DDCzTrz are shown in Figure S1a,b (Supporting Information). PL quantum yields of DCzTrz and DDCzTrz in toluene were 0.43 and 0.66, respectively.

Thermal stability of the synthesized TADF emitters was investigated because thermal stability is closely related with

the device stability. Differential scanning calorimeter (DSC) and thermogravimetric analyzer (TGA) data of DCzTrz and DDCzTrz are shown in Figure S2a,b (Supporting Information). DCzTrz and DDCzTrz showed glass transition temperatures of 160 °C and 218 °C, which was high enough to provide long-term stability during device operation. Thermal decomposition temperatures were 397 °C and 493 °C for DCzTrz and DDCzTrz, respectively. From these thermal analysis results, it can be assumed that the two TADF emitters possess good thermal stability for stable device operation.

Transient and time-resolved PL characterization of DCzTrz and DDCzTrz was conducted to identify delayed fluorescent behavior of DCzTrz and DDCzTrz. Transient PL decay curves of DCzTrz and DDCzTrz are shown in Figure 1c. In addition to sharp prompt fluorescence, delayed emission with a decay time of 3.1 and 2.8 μ s was observed in the DCzTrz and DDCzTrz emitters, respectively. This indicates that delayed emission contributes to the light emission of DCzTrz and DDCzTrz by delayed fluorescence process. Time-resolved PL spectra of DCzTrz and DDCzTrz before and after applying delay time of 14 μ s confirmed the delayed emission of DCzTrz and DDCzTrz because exactly the same PL spectra were obtained before and after applying delay time (Figure 1d). The delayed emission can be assumed to be singlet emission by delayed fluorescence process.

Delayed fluorescence behavior of DCzTrz and DDCzTrz confirmed from the transient and time-resolved PL measurement allowed the fabrication of blue TADF OLEDs by doping the emitters in the bis[2-(diphenylphosphino)phenyl]ether oxide (DPEPO) matrix. Figure 2a,b plot the current density and luminance dependence on the driving voltage of the TADF devices

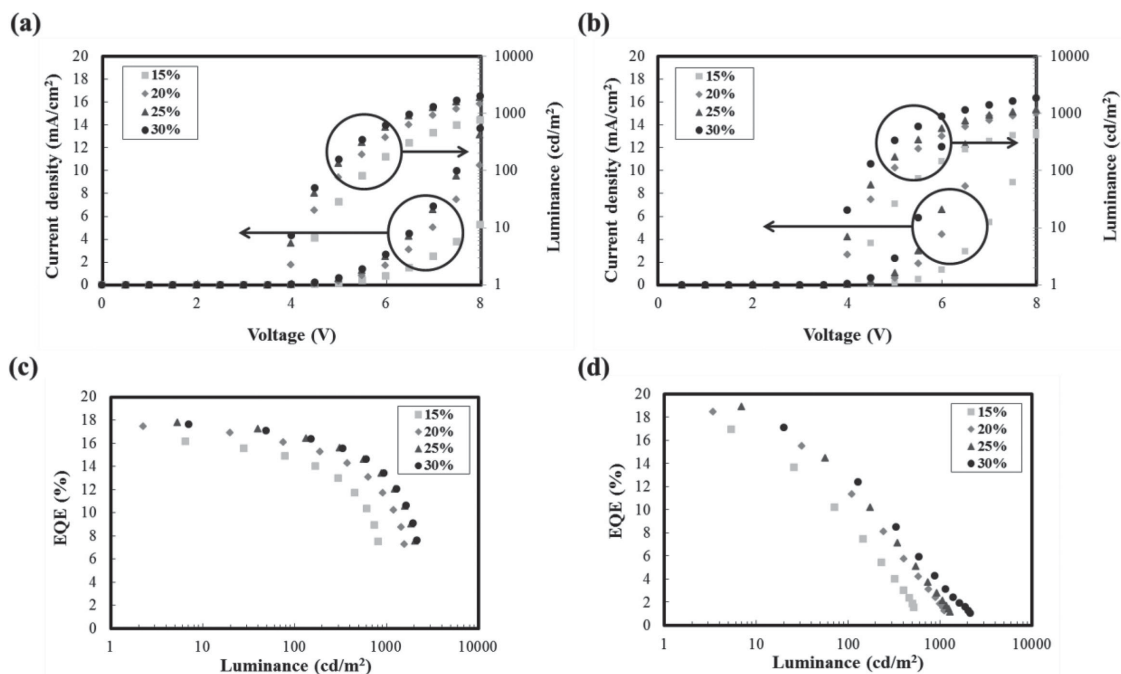


Figure 2. Current density–voltage–luminance curves of DPEPO:DCzTrz devices (a) and DPEPO:DDCzTrz devices (b) according to doping concentration of the dopant materials. Quantum efficiency–luminance curves of DPEPO:DCzTrz devices (c) and DPEPO:DDCzTrz devices (d) according to doping concentration of the dopant materials.

at doping concentrations varied from 15% to 30%. Relative increase of the current density and luminance by increasing the doping concentration was observed in the two devices, which can be explained by facile hole injection as can be inferred from the energy-level diagram in Figure S3 (Supporting Information). Hole injection from mCP hole transport layer to DPEPO is prevented by the HOMO gap of 0.7 eV between mCP and DPEPO, which renders hole injection from mCP to DCzTrz or DDCzTrz directly. Therefore, holes should be carried by the DCzTrz or DDCzTrz emitters and the hole movement is greatly assisted by the TADF emitters at high doping concentration due to easy hopping of hole carriers. Similar current density dependence on the doping concentration was observed in the two TADF devices. The higher current density of the DDCzTrz device than that of the DCzTrz device may be due to facile hole hopping between DDCzTrz because more hole transport-type carbazole units were included in the backbone structure. The rather low maximum luminance of the two devices is due to low electron mobility and poor stability of TSPO1 electron transport layer. It is possible to increase the maximum luminance if high mobility and thermally stable electron transport material with a high triplet energy is used.

Quantum efficiency–luminance relationship of the DCzTrz and DDCzTrz TADF OLEDs is displayed in Figure 2c,d. High doping of the TADF emitters leads to high quantum efficiency by balanced hole and electron density in the emitting layer as can be presumed from the high current density at high doping concentration. Maximum quantum efficiencies of DCzTrz and DDCzTrz devices were 17.8% and 18.9% at 25% doping concentration, respectively. The maximum quantum efficiency was obtained at high doping concentration in the two devices by optimized charge balance at high doping concentration. At low doping concentration, charge balance is poor due to low hole density and the maximum quantum efficiency was low. In addition to the optimized charge balance at high doping concentration, activated delayed fluorescence of the DCzTrz and DDCzTrz is responsible for the high quantum efficiency of the DCzTrz and DDCzTrz devices. The quantum efficiency of the two TADF devices was not greatly affected by the doping concentration at doping concentrations above 20%. The relatively high quantum efficiency of the DDCzTrz device to that of the DCzTrz device is caused by higher PL quantum yield of DDCzTrz than that of DCzTrz.

The rather serious efficiency roll-off of the device is mainly due to long excited state lifetime of the emitters and unipolar

character of DPEPO host material. The excited state lifetime of DCzTrz and DDCzTrz for delayed emission is 3.1 and 2.8 μ s, respectively. The long excited state lifetime induces triplet–triplet quenching, triplet–polaron quenching, and singlet–triplet quenching. The exciton quenching is significant at high current density and efficiency is reduced at high current density. The other reason is the unipolar transport character of DPEPO. DPEPO is an electron transport-type host material and the hole and electron balanced is disrupted at high current density because of poor hole transport character of DPEPO. Even though holes are injected at low current density, the poor hole transport character of DPEPO induces hole accumulation and hole injection is hindered. Therefore, electron density is high and hole density is low at high current density, which induces efficiency decrease at high current density. This problem can be solved by using bipolar host materials and TADF emitters with short excited state lifetime.

Electroluminescence (EL) spectra of DCzTrz and DDCzTrz devices are displayed in Figure 3a,b. EL emission peaks of DCzTrz and DDCzTrz were 459 and 467 nm, respectively, which coincided with the trend of the PL spectra. The EL spectra of the DDCzTrz device was shifted to long wavelength by the strong donor character and extended conjugation of DDCzTrz. The short-wavelength emission assigned deep blue emission color coordinates of (0.15, 0.15) and (0.16, 0.22) to the DCzTrz and DDCzTrz devices, respectively. Color coordinates of each device at 15% doping concentration were (0.15, 0.14) and (0.16, 0.22), respectively. Table 1 shows a summary of all device performances of DCzTrz and DDCzTrz deep blue TADF devices.

The lifetime of the DCzTrz and DDCzTrz devices was measured to assess the stability of the blue TADF devices. Relative luminance plot against driving time of the TADF devices is presented in Figure 4. Initial luminance of the device was 500 cd m^{-2} . In the lifetime measurement, DCzTrz and DDCzTrz were doped in the mCBP host at a doping concentration of 10% due to instability of the DPEPO host. Basic device performances are summarized in Figure S4 (Supporting Information). The quantum efficiency of the DCzTrz and DDCzTrz devices for lifetime measurement was not high because low triplet energy hole and electron transport materials were used due to unavailability of stable high triplet energy charge transport materials. The lifetime of the DCzTrz and DDCzTrz devices was compared with that of blue phosphorescent OLEDs with mCBP:tris[1-(2,4-diisopropyl)benzo[b,d]furan-3-yl]-2-phenylimidazole] ($\text{Ir}(\text{dbi})_3$) emitting layer.^[17] The

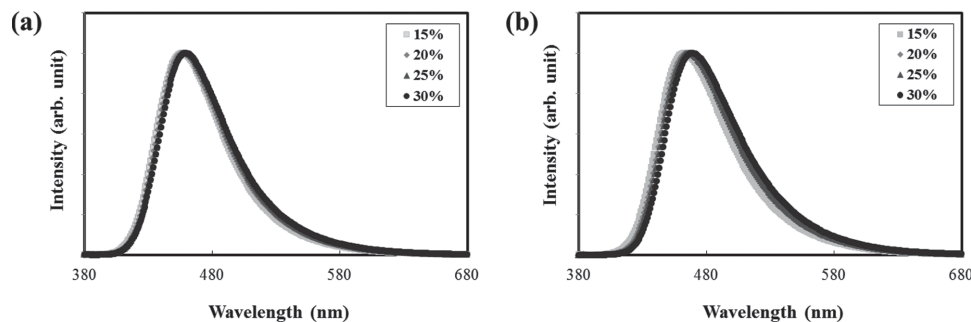


Figure 3. EL spectra of DPEPO:DCzTrz devices (a) and DPEPO:DDCzTrz devices (b) according to doping concentration of the dopant materials. EL spectra were collected at 500 cd m^{-2} .

Table 1. Summarized device performances of the DCzTrz and DDCzTrz devices at different doping concentrations.

| Devices | Maximum | | | 500 [cd m ⁻²] | | | Voltage [V] | Color coordinate |
|---------------|----------------------|--|--|---------------------------|--|--|-------------|------------------|
| | QE ^{a)} [%] | PE ^{b)} [lm W ⁻¹] | CE ^{c)} [cd A ⁻¹] | QE ^{a)} [%] | PE ^{b)} [lm W ⁻¹] | CE ^{c)} [cd A ⁻¹] | | |
| DCzTrz (15%) | 16.6 | 20.9 | 23.4 | 11.4 | 8.0 | 18.1 | 7.1 | (0.15,0.14) |
| DCzTrz (20%) | 17.5 | 22.0 | 25.5 | 13.7 | 11.0 | 21.8 | 6.2 | (0.15,0.15) |
| DCzTrz (25%) | 17.8 | 22.4 | 26.8 | 14.9 | 12.7 | 23.7 | 5.9 | (0.15,0.16) |
| DCzTrz (30%) | 17.6 | 22.2 | 26.9 | 15.0 | 13.0 | 23.7 | 5.8 | (0.16,0.17) |
| DDCzTrz (15%) | 16.9 | 19.2 | 24.8 | 2.0 | 1.2 | 3.1 | 8.4 | (0.16,0.19) |
| DDCzTrz (20%) | 18.4 | 23.6 | 30.1 | 5.0 | 4.0 | 8.0 | 6.3 | (0.16,0.21) |
| DDCzTrz (25%) | 18.9 | 26.2 | 31.3 | 5.5 | 4.8 | 9.0 | 5.9 | (0.16,0.22) |
| DDCzTrz (30%) | 17.1 | 23.5 | 30.0 | 6.9 | 7.1 | 11.9 | 5.3 | (0.16,0.24) |

^{a)}QE, quantum efficiency; ^{b)} PE, power efficiency; ^{c)} CE, current efficiency.

lifetime values of DCzTrz, DDCzTrz, and Ir(dbi)₃ devices up to 80% of initial luminance were 5, 52, and 18 h, respectively. The lifetime of the DDCzTrz device was almost three times as long as that of the Ir(dbi)₃ device, which can be understood by the stable molecular structure of DDCzTrz as explained in the molecular design concept. This work is the first demonstration of stable blue TADF OLEDs. In particular, the lifetimes of the current blue TADF OLEDs were much longer than that of the blue triplet OLEDs.

There are several factors for the improved long-term stability of the synthesized TADF devices, which are mostly related with the material design of the TADF emitters. One key factor is the stable molecular structure of DCzTrz and DDCzTrz. The two TADF-dopants of DCzTrz and DDCzTrz were designed to develop stable blue TADF emitters and have mainly triazine and dicarbazolyphenyl units, which are stable building units of host materials. The calculated dihedral angles between triazine and phenyl of 3,5-dicarbazolyphenyl units were 0.7° and 1.3° in the DCzTrz and DDCzTrz emitters (Figure S5, Supporting Information), which are beneficial for the stability of the blue TADF devices because the peripheral dicarbazolyphenyl moieties can be stabilized by the conjugation with the central triazine moiety via the

completely planar structure.^[18] Generally, triplet emitters with phenylimidazole-based ligands have been reported as relatively stable blue phosphorescent dopant materials,^[17–19] but they bear poor stability problem due to weak bonding between Ir and nitrogen of imidazole. The small dissociation energy problem of the triplet emitters can be avoided in the DDCzTrz emitter because it contains only chemically stable aromatic moieties and the dihedral angles between the aromatic moieties are small. It was reported that one key factor for the stability of the OLEDs is material stability, which depends on the stability of the chemical bond.^[18] Therefore, the lifetime was almost tripled by using the mCBP:DDCzTrz emitting layer as an alternative high efficiency emitting layer of mCBP:Ir(dbi)₃. The short lifetime of the DCzTrz device is due to blue-shifted high energy emission of the DCzTrz, which can degrade the device quickly.

The other factor is stability of DCzTrz and DDCzTrz under exciton formation. DCzTrz and DDCzTrz have well-separated HOMO and LUMO distribution, which means that positive polarons would be found in the dicarbazolyphenyl moieties and negative polarons would exist in the triazine moiety. It was already demonstrated in several works that carbazole derivatives are stable under positive polaron formation, while triazine derivatives are stable under negative polaron formation.^[18,20] Therefore, both positive and negative polarons are stabilized in the DCzTrz and DDCzTrz emitters, enhancing the lifetime of the TADF devices. Another factor is thermal stability of DCzTrz and DDCzTrz. Thermal stability, which is expressed as the *T_g* of the materials, is critical to the device lifetime because low *T_g* material can be crystallized or deformed during device operation. In the case of DCzTrz and DDCzTrz, the *T_g* was 160 °C and 218 °C, which is beneficial for the lifetime of the devices.

As mentioned above, planar molecular structure for bond stability, stability under exciton formation, and thermal stability contributed to the three times longer lifetime of the blue TADF devices than that of the blue phosphorescent OLEDs. From the results described above, it can be concluded that the blue TADF devices can provide similar quantum efficiency level to phosphorescent OLEDs and better lifetime than phosphorescent OLEDs by proper design of the TADF emitters. However, the lifetime of the current blue TADF OLEDs is much shorter

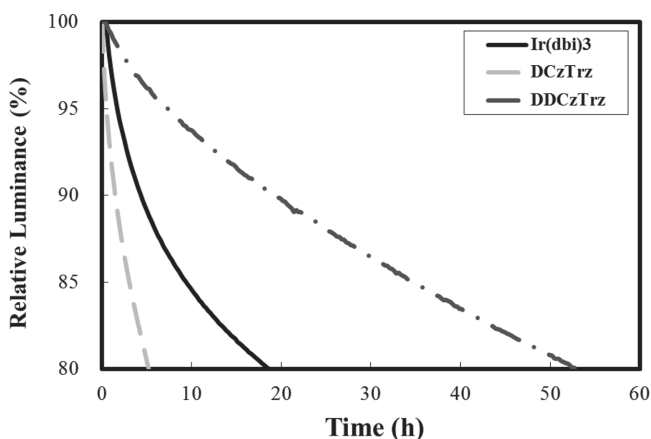


Figure 4. Lifetime curves of mCBP:Ir(dbi)₃, mCBP:DCzTrz, and mCBP:DDCzTrz devices. Lifetime was measured at an initial luminance of 500 cd m⁻².

than that of red and green devices because of lack of stable host materials with a triplet energy high enough for the blue TADF emitters. Although mCBP was used in this work, it is not the best material for blue TADF dopant because of rather low triplet energy. The lifetime of the blue TADF device can be improved further by developing stable host materials with a high triplet energy.

In conclusion, two blue TADF emitters, DCzTrz and DDCzTrz, were synthesized as stable TADF emitters for high efficiency and long lifetime. DDCzTrz was efficient as a blue TADF emitter and could show high maximum quantum efficiency of 18.9% and lifetime of 52 h up to 80% of initial luminance at 500 cd m⁻², which was almost three times as long as that of blue phosphorescent OLEDs. Therefore, the triazine- and dicarbazolyphenyl-based TADF design can pave a way to develop stable blue TADF emitters for long lifetime and high efficiency.

Experimental Section

Synthesis: Synthetic methods of DCzTrz and DDCzTrz were added in Supporting Information.

Device Fabrication: All devices reported in this work were fabricated using a thermal evaporator with a vacuum pressure of 1.0×10^{-6} torr. Organic layers were grown on a 120-nm-thick indium tin oxide substrate cleaned using deionized water and hot 2-propanol at an order of poly(3,4-ethylenedioxythiophene):poly(styrenesulfonate) (PEDOT:PSS, 60 nm), 4,4'-cyclohexylidenebis[N,N-bis(4-methylphenyl)aniline] (10 nm), *tris*(4-carbazol-9-ylphenyl)amine (10 nm), 1,3-bis(*N*-carbazolyl)benzene (10 nm), DPEPO:DCzTrz, or DPEPO:DDCzTrz, diphenylphosphine oxide-4-(triphenylsilyl)phenyl (5 nm), 1,3,5-tris(*N*-phenylbenzimidazole-2-yl)benzene (30 nm), LiF (1 nm), and Al (200 nm). The device structure of the blue devices for lifetime measurement was ITO (120 nm)/*N,N'*-diphenyl-*N,N'*-bis-[4-(phenyl-*m*-tolyl-amino)-phenyl]-biphenyl-4,4'-diamine (60 nm)/*N,N,N',N'*-tetra[(1,1'-biphenyl)-4-yl]-(1,1'-biphenyl)-4,4'-diamine (30 nm)/mCBP:Ir(dbi)₃ or mCBP:DCzTrz or mCBP:DDCzTrz (25 nm)/LG201 (35 nm)/LiF (1 nm)/Al (200 nm). Encapsulation of the devices was finished inside glove box after device fabrication.

Measurements: Electrical characteristics of the fabricated devices were analyzed using Keithley 2400 source measurement unit and light emission characteristics were measured using CS 2000 spectroradiometer. Lifetime analysis of the TADF devices was done at a constant current mode at an initial luminance of 500 cd m⁻².

Supporting Information

Supporting Information is available from the Wiley Online Library or from the author.

Acknowledgements

This research was supported by Basic Science Research Program through the National Research Foundation of Korea (NRF) funded by the Ministry of Education, Science, and Technology (2013R1A1A2A007991) and Ministry of Science, ICT, and Future Planning (2013R1A2A2A01067447) and development of red and blue OLEDs with external quantum efficiency over 20% using delayed fluorescent materials funded by MOTIE.

Received: January 18, 2015

Revised: February 12, 2015

Published online:

- [1] H. Uoyama, K. Goushi, K. Shizu, H. Nomura, C. Adachi, *Nature* **2012**, *492*, 234.
- [2] J. W. Sun, J. H. Lee, C. K. Moon, K. H. Kim, H. S. Shin, J. J. Kim, *Adv. Mater.* **2014**, *26*, 5684.
- [3] Q. Zhang, B. Li, S. Huang, H. Nomura, H. Tanaka, C. Adachi, *Nat. Photon.* **2014**, *8*, 326.
- [4] A. Endo, K. Sato, K. Yoshimura, T. Kai, A. Kawada, H. Miyazaki, C. Adachi, *Appl. Phys. Lett.* **2011**, *98*, 083302.
- [5] G. Mehes, H. Nomura, Q. Zhang, T. Nakagawa, C. Adachi, *Angew. Chem. Int. Ed.* **2012**, *51*, 11311.
- [6] T. Nakagawa, S. Y. Ku, K. T. Wong, C. Adachi, *Chem. Commun.* **2012**, *48*, 9580.
- [7] S. Y. Lee, T. Yasuda, H. Nomura, C. Adachi, *Appl. Phys. Lett.* **2012**, *101*, 093306.
- [8] H. Tanaka, K. Shizu, H. Miyazaki, C. Adachi, *Chem. Commun.* **2012**, *48*, 11392.
- [9] Q. Zhang, J. Li, K. Shizu, S. Huang, S. Hirata, H. Miyazaki, C. Adachi, *J. Am. Chem. Soc.* **2012**, *134*, 14706.
- [10] K. Sato, K. Shizu, K. Yoshimura, A. Kawada, H. Miyazaki, C. Adachi, *Phys. Rev. Lett.* **2013**, *110*, 247401.
- [11] J. Lee, K. Shizu, H. Tanaka, H. Nomura, T. Yasuda, C. Adachi, *J. Mater. Chem. C.* **2013**, *1*, 4599.
- [12] K. Nasu, T. Nakagawa, H. Nomura, C. J. Lin, C. H. Cheng, M. R. Tseng, T. Yasuda, C. Adachi, *Chem. Commun.* **2013**, *49*, 10385.
- [13] S. Y. Lee, T. Yasuda, Y. S. Yang, Q. Zhang, C. Adachi, *Angew. Chem.* **2014**, *126*, 6520.
- [14] H. Wang, L. Xie, Q. Peng, L. Meng, Y. Wang, Y. Yi, P. Wang, *Adv. Mater.* **2014**, *26*, 5198.
- [15] H. Nakanotani, K. Masui, J. Nishide, T. Shibata, C. Adachi, *Sci. Rep.* **2013**, *3*, 2127.
- [16] Y. J. Cho, J. Y. Lee, *Adv. Mater.* **2014**, *24*, 4050.
- [17] J. Zhuanga, W. Lib, W. Sub, Y. Liuc, Q. Shena, L. Liaoc, M. Zhou, *Org. Electron.* **2013**, *14*, 2596.
- [18] S. Schmidbauer, A. Hohenleutner, B. Konig, *Adv. Mater.* **2013**, *25*, 2114.
- [19] Y. Zhang, J. Lee, S. R. Forrest, *Nat. Commun.* **2014**, *5*, 5008.
- [20] H. Nak anotani, K. Masui, J. Nishide, T. Shibata, C. Adachi, *Sci. Rep.* **2013**, *3*, 2127.